

Light amplification and laser emission in conjugated polymers

Axel Schülzgen

Christine Spiegelberg

Michael M. Morrell, MEMBER SPIE

Sergio B. Mendes, MEMBER SPIE

University of Arizona

Optical Sciences Center

Tucson, Arizona 85721

E-mail: axel@u.arizona.edu

Pierre-Marc Allemand

Donelly Corporation

Tucson, Arizona 85721-1108

Yutaka Kawabe

University of Arizona

Optical Sciences Center

Tucson, Arizona 85721

Makoto Kuwata-Gonokami

University of Tokyo

Department of Applied Physics

Bunkyo-Ku, Tokyo 113

Japan

Seppo Honkanen, MEMBER SPIE

Mahmoud Fallahi, MEMBER SPIE

Bernard Kippelen

Nasser Peyghambarian, MEMBER SPIE

University of Arizona

Optical Sciences Center

Tucson, Arizona 85721

Abstract. We study optical gain and laser emission from semiconducting conjugated polymers after strong optical excitation with femtosecond laser pulses. Stimulated emission from few-hundred-nanometer thin films results in a sharp increase in emission intensity and emission line narrowing. Very large optical gain due to the stimulated emission is measured directly by pump-probe spectroscopy. Using the large light amplification in these conjugated polymers, we demonstrated planar and ring lasers of very small sizes that are suitable for applications in integrated optics. Vertical cavity surface emitting lasers, distributed feedback through surface relief grating, and whispering-gallery mode emission from ring resonators are demonstrated. © 1998 Society of Photo-Optical Instrumentation Engineers. [S0091-3286(98)01204-5]

Subject terms: conjugated polymers; laser emission; optical gain; resonator configurations.

Paper INT-12 received Oct. 1, 1997; accepted for publication Oct. 20, 1997.

1 Introduction

Conjugated polymer semiconductors have attracted attention lately for device applications in areas that are traditionally domains of inorganic semiconductors, such as electronic devices (e.g., diodes, field-effect transistors) and photonic devices, including holographic storage, light modulators, and light-emitting diodes (LEDs). The structural flexibility, easy processing, and low cost of polymers make polymer devices competitive. One of the most useful properties for optical applications is that the absorption and emission of conjugated polymers can be tuned over the whole visible spectrum by changing their chemical structure.

Recently, photoluminescence (PL) line narrowing and stimulated emission (SE) have been reported in a variety of conjugated polymers.¹⁻⁶ The prospect of compact electrically pumped polymer lasers using their semiconductor properties is exciting. First reports on the emission properties of optically pumped polymer films in microcavity structures showed increased directionality and threshold behavior in the mode structure, indicating feedback effects of

the cavity.^{1,5} Very recently, using an improved resonator configuration, we have been able to obtain unambiguous features of laser emission such as directionality close to the diffraction limit and a high degree of polarization.⁷

In this paper, we focus on the optical properties of thin solid-state films of semiconducting polymers and related microstructures under high excitation conditions. Femtosecond spectroscopy is used to study the optical response and its dynamics after excitation with short optical pulses. We show that very large optical gain and stimulated emission can be achieved in extremely thin polymer films. The large light amplification per unit length allows laser action to occur with small interaction lengths between the conjugated polymer and the electromagnetic light field. Small planar and ring laser configurations can provide the optical feedback that makes these solid-state organic lasers particularly interesting for integrated optics applications. Under optical excitation we demonstrate threshold behavior of the laser modes in various microcavity configurations and discuss characteristic features of the laser output.

2 Experimental

Films of 100- to 500-nm thickness of the semiconducting conjugated polymer BEH:PPV [poly(2,5-bis(2'-ethylhexyloxy)-1,4-phenylenevinylene)⁸] were spin-coated from xylene solution onto different substrates. For PL and optical gain measurements the polymer films were deposited on microscope slides. The polymers were also coated directly onto various structured substrates to form microcavity devices.

For surface-emitting planar Fabry-Perot resonators, dielectric mirrors were produced by electron-beam deposition. Each mirror consisted of a stack of 21 alternating quarterwave layers of materials with low (SiO_2) and high (TiO_2) refractive index. These mirrors exhibited low losses and extremely high reflectivities ($>99\%$) in the wavelength region of optical gain in the polymer. By spin-coating the polymer onto one of the dielectric mirrors and properly adjusting the second mirror, we produced a low-loss, high- Q planar microcavity of about $9\text{-}\mu\text{m}$ optical thickness. For distributed feedback laser structures, we defined surface relief gratings with periods of $\Lambda = 500\text{ nm}$. The grating was defined using holography techniques and was etched into a glass substrate by plasma etching. The polymer was deposited on top of this grating.

Additionally, we present results for two different ring resonators. The first microring was formed by the surface tension of a polymer droplet encircling an optical fiber of $56\text{-}\mu\text{m}$ diameter. The second was formed by a Si_3N_4 waveguide structure on oxidized Si with a ring diameter of $35\text{ }\mu\text{m}$. The waveguide structure was covered with an additional 50 nm of oxidized Si with an opening at the position of the ring resonator. A 200-nm -thick polymer film was spin-coated on the waveguide device. In this case, the light output was observed from a channel waveguide, which was designed to have a small coupling ($<5\%$) to the ring resonator.

To excite the polymer films optically we used an amplified colliding pulse mode-locked (CPM) laser system providing tunable pulses of 100-fs duration. The central wavelength of the excitation pulses, 555 nm , was in resonance with the $\pi\text{-}\pi^*$ absorption band of BEH:PPV. Additionally, a spectrally broad ($>100\text{ nm}$) probe pulse was generated by the same laser system that was used to measure the dynamics of absorption changes and light amplification in a pump-probe setup. Taking careful account of linear and quadratic chirp in the broad probe continuum, we analyzed the dynamics of light amplification with a time resolution of the order of the pulse length. For the waveguide ring resonator we present results under quasistationary excitation conditions using 7-ns pulses from a frequency-doubled Nd:YLF laser at 524 nm . The optical signals were detected by an optical multichannel analyzer with a spectral resolution better than 0.3 nm . All experiments are carried out at room temperature.

3 Photoluminescence and Stimulated Emission

The energy-level structure of the conjugated polymer that dominates absorption and emission properties is schematically shown in Fig. 1. Characteristic of organic materials, each electronic level is associated with a set of vibrational energy levels that are spaced very closely compared to the

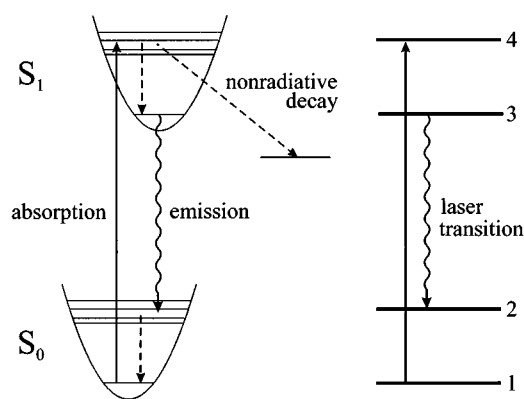


Fig. 1 Schematic drawing of the energy-level diagram of an organic material (left) and the corresponding approximate four-level picture (right).

electronic energy level spacing. Absorption of radiation takes place from the bottom of the S_0 level to one of the S_1 levels. From there, the excitation nonradiatively decays very quickly down to the bottom of S_1 or to energy levels that are not coupled radiatively to S_0 . Radiative emission is accompanied by the transition from the bottom of S_1 to one of the vibronic levels in S_0 . This energy transition scheme leads to the well-known mirror-image-like relation between absorption and emission spectra that is typical for organic molecules and also for semiconducting conjugated polymers such as BEH:PPV. The very fast decay from higher vibrational levels to the bottom of S_1 and S_0 leads to an energy-level scheme that is similar to a four-level system (right-hand side in Fig. 1), known to be well suited for laser applications.

Figure 2 shows the normalized PL spectra of BEH:PPV for three different pump intensities. The arrow marks the excitation wavelength and its position in the $S_0 \rightarrow S_1$ absorption manifold that is inhomogeneously broadened due to chain segments with different effective conjugation lengths. The PL at low excitation (curve i in Fig. 2) is due

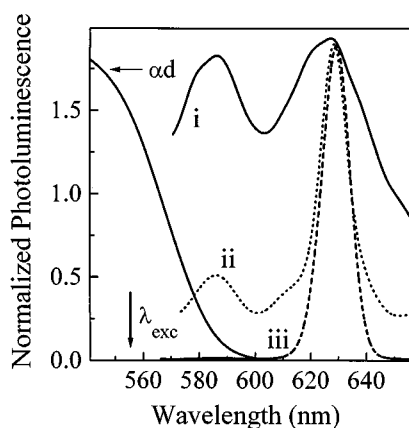


Fig. 2 Normalized PL spectra of a 100-nm BEH:PPV film after excitation with 100-fs pulses ($\lambda_{exc} = 555\text{ nm}$) and excitation fluences of (i) 30 , (ii) 50 , and (iii) $120\text{ }\mu\text{J}/\text{cm}^2$. For comparison the absorption spectrum is also given.

to the recombination of singlet excitons and exhibits a dominant vibrational structure with an energy spacing of about 150 meV that corresponds to the frequency of phenylene backbone vibrations. A closer look indicates additional vibronic substructures. It has been shown that excitons not only undergo very fast vibrational relaxation, but also migrate efficiently to chain segments of longer conjugation length.^{9–12} Relaxation and migration within a few hundred femtoseconds result in a red shift of the PL relative to the absorption and emission lines, which are substantially narrower than those in absorption. Therefore, the low-excitation PL spectrum is dominated by excitons at the longest conjugation segments. In this regime, we find a quantum efficiency of only 5% measured with an integrating sphere, i.e., 95% of the excited excitons decay via the nonradiative recombination channels that are indicated in Fig. 1. This is in agreement with time-resolved PL measurements, where we observed a nonradiative decay time of about 50 ps, while the time constant for radiative recombination is about 1.2 ns.⁹

On increasing the excitation intensity, the initially broad PL spectrum collapses into a single line, centered at 630 nm, of about 9-nm width (curve iii in Fig. 2). This transition occurs at about $50 \mu\text{J}/\text{cm}^2$, corresponding to an average exciton density of $5 \times 10^{18} \text{ cm}^{-3}$. Simultaneously, the emission intensity at 630 nm increases dramatically, as does the quantum efficiency. The reason is that above $50 \mu\text{J}/\text{cm}^2$ the exciton recombination is dominated by SE. In contrast to the constant rate for spontaneous emission, the probability for SE is proportional to the light intensity at the given wavelength. If the number of spontaneously emitted photons is large enough, this radiation can stimulate the recombination with a probability higher than that for the nonradiative decay. In turn, the number of photons is further increased and SE becomes even more probable, leading to a complete bypass of all nonradiative recombination channels. At about $100 \mu\text{J}/\text{cm}^2$ the dominance of SE leads to a quantum efficiency of almost 100% while the emission intensity decays faster than 10 ps.¹⁰

4 Optical Gain

The measured PL line narrowing and fast SE indicate large optical gain in the thin polymer films. The strong anisotropy in conjugated polymers due to the molecule arrangement results in large dipole moments and, correspondingly, absorption coefficients on the order of 10^5 to 10^6 cm^{-1} . According to Einstein's theory, gain coefficients can be expected that are comparable to the absorption coefficients provided that we can create a large inversion between the initial and the final state of the stimulation process.

In Fig. 3 we present the measured changes of the optical response of a 190-nm-thick BEH:PPV film in the spectral region around the band-gap energy of the semiconducting polymer for the case of optimized temporal overlap ($\Delta t = 0$) between the exciting pump pulse (555 nm) and the probe pulse. The spectra are shown for three different excitation intensities above the SE threshold. At shorter wavelengths, where the material is absorbing (left-hand side of Fig. 3), the relative absorption bleaching ($-\Delta\alpha/\alpha_{\text{lin}}$) is plotted, while at longer wavelength (right-hand side of Fig. 3) the net optical gain ($-\Delta\alpha - \alpha_{\text{lin}}$) d is

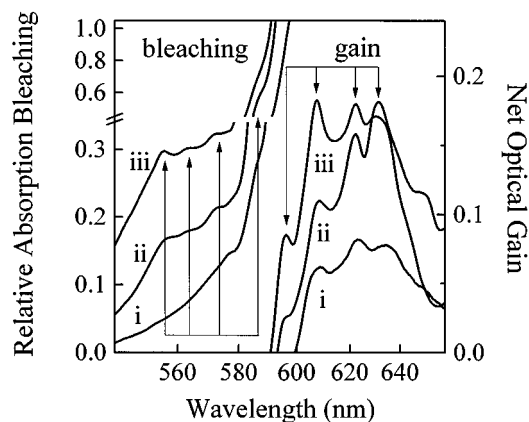


Fig. 3 Relative absorption bleaching $-\Delta\alpha/\alpha_{\text{lin}}$ (left) and net optical gain $(-\Delta\alpha - \alpha_{\text{lin}})d$ (right) measured in the absorbing and the transparent regions of a 190-nm BEH:PPV film, respectively. The data for three different pump pulse fluences (i: 100, ii: 400, iii: $1000 \mu\text{J}/\text{cm}^2$) are taken at zero delay between pump and probe pulses. Arrows indicate the transition energies in absorption and stimulated emission.

shown, where d is the sample thickness, α_{lin} the linear absorption coefficient, and $\Delta\alpha$ the change in absorption in the presence of the pump beam. To obtain α_{lin} and $\Delta\alpha$ we measured the spectra of the incident probe pulse (I_0), of the transmitted probe pulse without pump [$I_t = I_0 \exp(-\alpha_{\text{lin}}d)$], and of the transmitted probe pulse with pump beam [$I_t = I_0 \exp[-(\alpha_{\text{lin}} + \Delta\alpha)d]$]. Below and above the onset of the linear absorption we observe a negative $\Delta\alpha$, i.e., in the presence of pump pulses, the absorption is reduced (bleached) at shorter wavelengths but still exists as long as $-\Delta\alpha/\alpha_{\text{lin}} < 1$. At longer wavelengths where $-\Delta\alpha/\alpha_{\text{lin}} > 1$ ($-\Delta\alpha - \alpha_{\text{lin}} > 0$) the probe light is amplified during the interaction with the polymer film due to stimulated emission.

Absorption bleaching is observed at the spectral position of the pump laser (555 nm) and in a broad spectral region that covers more than 180 meV around this wavelength. Three different transitions can be distinguished in the energetic region below the excitation wavelength. These transitions can be assigned to different vibronic levels in the S_1 band. Since absorption bleaching reflects the exciton population in these levels, the spectra provide evidence for very fast relaxation (< 150 fs) to the bottom of the S_1 band and successive filling of higher vibronic levels at higher excitation intensities. However, the relative bleaching, i.e., the occupation, is always the largest for the level with the lowest energy.

The gain spectra on the right-hand side show very large optical amplification in a broad spectral region (> 150 meV) starting just below the band-gap energy. A net gain of 0.19 translates into a large gain coefficient of 10^4 cm^{-1} . This is by far the largest value reported for a semiconducting polymer. It can be clearly seen in the gain spectra that light amplification is due to SE of at least four distinguishable optical transitions, each with a full width at half maximum of about 8 nm. Since their energy separation displays mirror symmetry with respect to the transitions observed in absorption bleaching, they can be assigned to

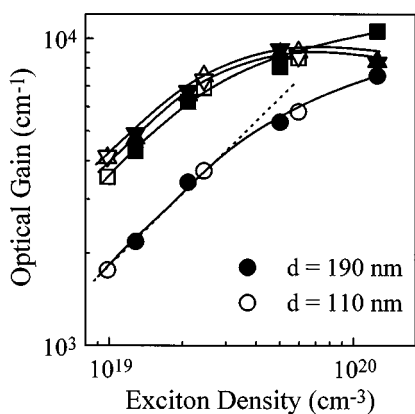


Fig. 4 Dependence of the optical gain coefficients ($\Delta t=0$) on the excited exciton density. The gain at four different wavelengths is plotted: point-up triangles: 630 nm; point-down triangles: 621 nm; squares: 609 nm; circles: 595 nm. Open and closed symbols are measured at a 110-nm film and a 190-nm film, respectively.

transitions from the bottom of the S_1 band to the vibronic levels in the S_0 band. Note that a superposition of the same transitions yields the low-density PL spectrum of Fig. 2, as we have shown recently.⁶ Increasing the excitation results in larger amplification. Furthermore, higher vibrational levels of S_1 become more and more occupied, leading to a stronger increase of the corresponding gain at shorter wavelength.

Figure 4 shows the gain coefficients ($\Delta t=0$) as a function of the excited exciton density taken at the four transition wavelengths and from two films of different thicknesses. The data show that the measured gain values are intrinsic material parameters that do not depend on film thickness or sample geometry. Up to exciton densities of $3 \times 10^{19} \text{ cm}^{-3}$ the gain increases linearly with density at all four transitions. We find a common cross section (gain per exciton per cubic centimeter) for SE of $2 \times 10^{16} \text{ cm}^2$, which indicates the possibility of considerable amplification even at densities below the threshold where SE dominates the emission from the thin films. Above an exciton density of $3 \times 10^{19} \text{ cm}^{-3}$ the gain at longer wavelength starts to saturate because of the finite density of states available at the bottom of S_1 . At 595 nm the gain can further increase due to the contributions from transitions starting at higher vibrational levels of S_1 , which become more and more occupied.

Decay curves of absorption bleaching at 575 nm and optical gain at 621 nm are shown in Figs. 5(a) and 5(b) for two different intensities. The main figures show the decay on a semilogarithmic scale at early times. In the insets we plot the temporal development for longer times and on a linear scale. At the excitation fluences of 100 and $150 \mu\text{J}/\text{cm}^2$ no significant gain saturation has yet occurred. Absorption bleaching [Fig. 5(a)] and optical gain [Fig. 5(b)] display the same dynamics. This behavior indicates that the same optically excited species are responsible for absorption bleaching and amplification by SE. Both signals reflect the dynamics of the excited exciton density. The decay of bleaching and gain is clearly nonexponential. Initially the absorption changes decay very fast, on a 100-fs

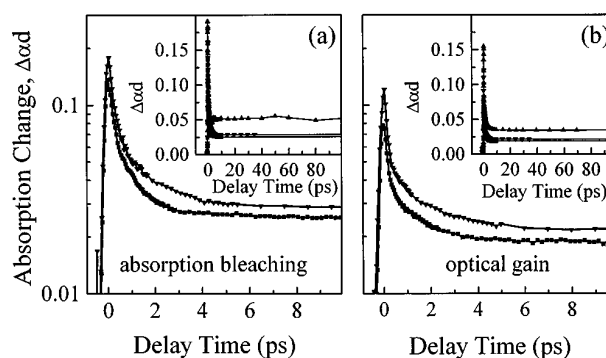


Fig. 5 Decay curves of the excitation-induced absorption change at two different wavelength representing (a) absorption bleaching at 575 nm and (b) optical gain at 621 nm. Data for excitation fluences of $100 \mu\text{J}/\text{cm}^2$ (squares), $150 \mu\text{J}/\text{cm}^2$ (point-down triangles), and $400 \mu\text{J}/\text{cm}^2$ (point-up triangles) are plotted. The insets show the same signals on a longer time scale.

scale. After a few hundred femtoseconds the decay slows down and the signals decrease with a characteristic time constant of about 2 ps. This can be explained in terms of a reduction of the excited-exciton density by SE. Since the probability for SE depends on the exciton density itself, the density is expected to decay nonexponentially and to slow down markedly for longer times (smaller densities). Additionally, we find a component of the absorption changes that persists for several hundred picoseconds without any significant decay. The magnitude of this plateau is found to be proportional to the initially excited density. Our results indicate that the long-lived component is due to localized excitons preferentially formed by initially excited excitons with large momenta that are able to move to localization sites. For laser applications we can exploit the fact that about 10% of the initial optical gain is still present after more than 500 ps.

5 Laser Action

The large optical gain makes semiconducting conjugated polymers promising candidates as new laser materials. For laser applications, however, the polymer as the active material has to be combined with a structure that provides optical feedback. Although electrically pumped laser diodes are the devices of choice for applications, optical pumping is a suitable method to study the properties of different laser structures. By studying the cavity emission it is sometimes difficult to decide whether or not the cavity emission should be called laser emission. Cavity modes can be seen in the low-density PL spectrum of any material embedded in a resonator. Laser action requires that the optical gain due to SE at least balance the total loss of the cavity structures. This condition leads to a thresholdlike increase of the cavity emission intensity when laser emission occurs. However, the interpretation of cavity-emission data using polymers as active material is additionally complicated in that a thresholdlike increase in emission intensity can also be seen from polymer films without any feedback (see Sec. 1) due to the onset of SE. The best argument for laser oscillation is to provide evidence for temporal and/or spatial coherence of the emission.

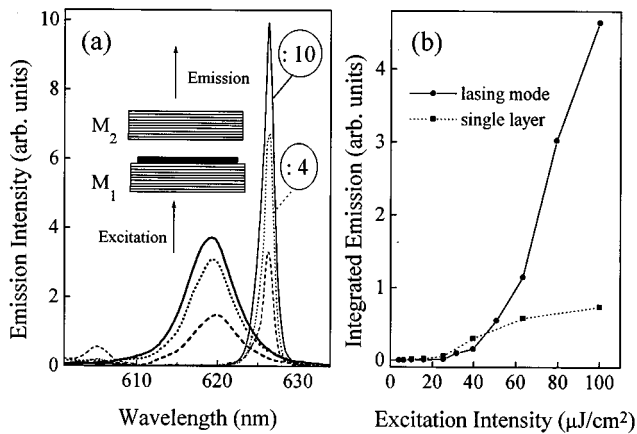


Fig. 6 (a) Emission spectra of a single BEH:PPV layer (thick lines) and a planar polymer cavity of 9- μm optical thickness (thin lines). The excitation intensities are 40 $\mu\text{J}/\text{cm}^2$ (dashed lines), 63 $\mu\text{J}/\text{cm}^2$ (dotted lines), and 100 $\mu\text{J}/\text{cm}^2$ (solid lines), respectively. In the inset the structure is shown schematically. (b) Spectrally integrated single-layer emission intensity and lasing cavity mode intensity as a function of pump laser fluence.

The most straightforward way to provide feedback is to design a cavity that uses two plane mirrors. Emission properties from such planar cavities under optical pumping have been reported recently.^{1,5,7} Figure 6(a) directly compares emission spectra from a thin BEH:PPV film outside and inside a cavity formed by highly reflective dielectric mirrors M_1 and M_2 . The mirrors are also designed to allow optical pumping through the mirror M_1 , which is characterized by 80% transmission at the excitation wavelength of 555 nm. In all cases shown in Fig. 6 the excitation is so strong that SE dominates the recombination. Simply removing M_2 allows an immediate study of the cavity effect.

Obviously, the emission properties are dramatically changed in the presence of the cavity. Whereas the single-layer emission shows the characteristic narrow 8-nm emission band centered at 620 nm, two longitudinal cavity modes at 605 and 626 nm dominate the cavity emission. For the single layer the spectral shape of the emission is almost the same for all three excitation intensities. In contrast, the intensity ratio between the cavity modes changes dramatically. A clear indication for laser emission from the 626-nm mode is given in Fig. 6(b), where we compare the intensity of the spectrally integrated thin-film emission with the intensity of the lasing mode at 626 nm. SE sets in at 25 $\mu\text{J}/\text{cm}^2$ (for both structures), whereas a clear lasing threshold occurs at 50 $\mu\text{J}/\text{cm}^2$. Above the threshold the laser emission increases linearly with the excitation, and the measured intensity clearly exceeds that from the film. Since the emission efficiency cannot be larger than 100%, the larger cavity output indicates high directionality of the laser emission, i.e., for the laser the entire emission falls into our detection cone of 10-deg half apex angle, whereas only about 10% of the almost isotropic single-film emission is detected.

Figure 7(a) shows that the whole laser emission is indeed concentrated in a cone of smaller than 3-deg half apex angle (63- $\mu\text{J}/\text{cm}^2$ excitation). This degree of directionality

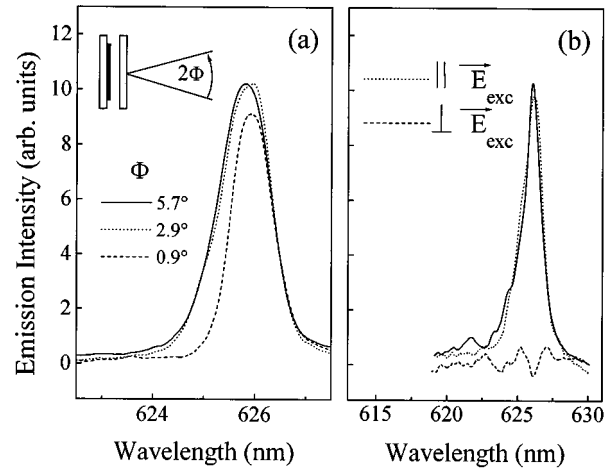


Fig. 7 (a) Detected planar cavity emission spectrum above the laser threshold for various apex angles Φ of the detection cone, indicating nearly diffraction-limited laser output. (b) Emission spectrum of the laser cavity detected without analyzer (solid line, normalized), with an analyzer parallel to the exciting laser (dotted line), and with an analyzer perpendicular to the exciting laser (dashed line), showing a polarization degree better than 50 : 1.

provides striking evidence for spatial coherence of the laser emission. Since the Huygens wavelets from different points all add up coherently, the beam divergence is nearly diffraction-limited. The presence of higher-order transverse modes is indicated by the intensity reduction on the high-energy side of the laser emission for the smallest aperture.⁷ Additional evidence for coherent laser emission is given by the high degree of polarization (better than 50 : 1) parallel to the polarization of the exciting laser [see Fig. 7(b), 55- $\mu\text{J}/\text{cm}^2$ excitation]. In contrast, neither the SE of the film nor the cavity emission at 605 nm has a noticeable degree of polarization.

An example of a distributed feedback resonator is shown in Fig. 8. Here the surface emission from a 200-nm BEH:PPV film deposited on top of a surface relief grating is shown. The exciting laser is focused to a stripe of 3-mm length and 50- μm width to get sufficient feedback by the grating. The optical feedback results in an emission line of only 3.5-nm width, which is considerably narrower than the 8-nm-wide SE band observed by exciting a part of the same film without a grating. The inset of Fig. 8 shows that we also observe a thresholdlike increase in emission intensity at about 40 $\mu\text{J}/\text{cm}^2$. However, it should be noted that this structure has not been optimized so far, and large scattering losses as well as a dependence on the spot position due to a nonuniform grating have also been observed.

Ring lasers are an alternative to cavity configurations with plane mirrors and gratings. Figure 9 shows the emission of a microring cavity formed by a thin polymer encircling an optical fiber of 56- μm diameter. It has been shown recently that this kind of structure forms a high-quality cavity for whispering-gallery modes (WGMs).^{13,14} These modes propagate around the edge of the coated fiber with a strong optical confinement in the gain material. Whereas in the previous study¹³ a laser dye dissolved in a polymer host provides the optical gain, we show in Fig. 9 that the gain in a conjugated polymer can also be sufficient to achieve laser

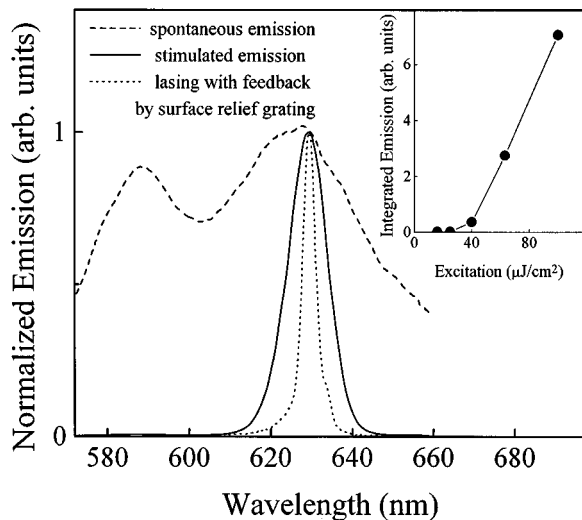


Fig. 8 Comparison of the emission spectra from a 200-nm BEH:PPV film: Spontaneous emission at low excitation (dashed line), stimulated emission without feedback (solid line), and laser emission with feedback provided by a surface relief grating (dotted line, $\Lambda=500$ nm). Inset: Integrated emission intensity of the laser structure as a function of excitation.

oscillations of the WGMs. For excitation below $25 \mu\text{J}/\text{cm}^2$ the emission is similar to the low-density PL without a particular mode structure. Supported by the optical gain in the BEH:PPV, the WGMs clearly dominate the emission above $30 \mu\text{J}/\text{cm}^2$, as can be seen in Fig. 9. They are only observed in a spectral region between 618 and 638 nm, where the gain is largest. The mode separation of 1.5 nm agrees well with the separation of the eigenvalues of the WGMs for a 56- μm -diam microring. The inset of Fig. 9 shows the emission intensity as a function of excitation.

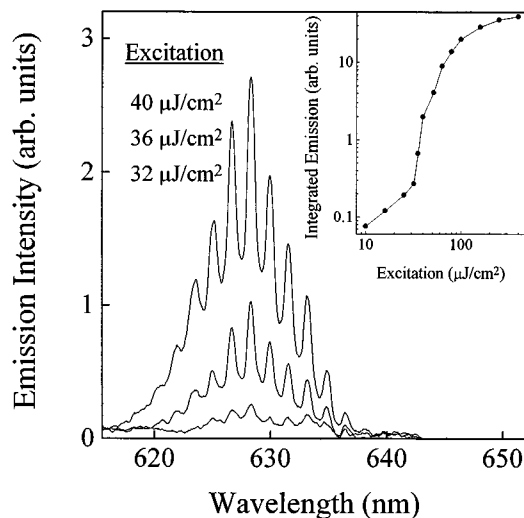


Fig. 9 Emission spectra from a polymer microring encircling an optical fiber of 56- μm diameter at three different excitation intensities. Lasing of whispering-gallery modes is found for excitation above $30 \mu\text{J}/\text{cm}^2$. Inset: Integrated emission intensity as a function of excitation.

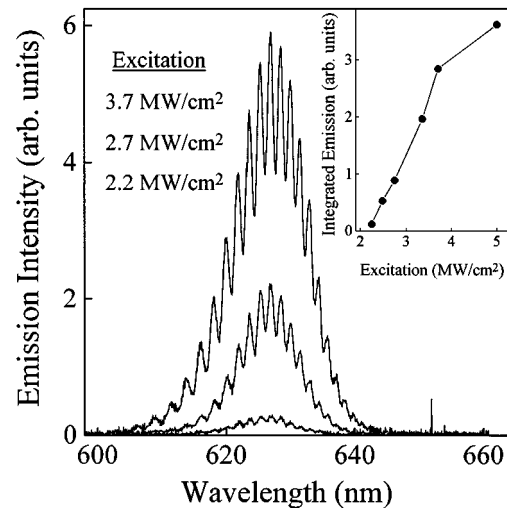


Fig. 10 Emission spectra of a waveguide ring resonator structure covered with a 200-nm BEH:PPV film for different excitation levels of the polymer layer. The spectra are observed at the output of a channel waveguide that is slightly coupled to the ring resonator. Inset: Spectrally integrated output of the straight waveguide as a function of optical excitation of the polymer film. The emission has been normalized to the excitation fluence.

The threshold for lasing of the WGMs is found to be $30 \mu\text{J}/\text{cm}^2$, and gain saturation sets in above $100 \mu\text{J}/\text{cm}^2$.

Figure 10 shows the emission of another ring cavity structure formed by a 100-nm BEH:PPV film deposited on a Si_3N_4 waveguide ring resonator. The waveguide is formed by a 25-nm-high and 9- μm -wide Si_3N_4 ridge on top of a 275-nm Si_3N_4 layer that is deposited on an oxidized Si substrate. Since the guided cavity mode reaches out into the polymer layer, optical gain in the polymer leads to amplification of light that is emitted into one of the ring cavity modes. The ring resonator is designed to have a small coupling to a channel waveguide. By detecting the output of the channel waveguide we can measure the laser emission without detecting any background from scattered pump light.

In Fig. 10 we show the output spectra of the channel waveguide after excitation of the polymer from the top with 7-ns pulses at 524 nm from a Nd:YLF laser. Increasing the excitation, we find a clear threshold in emission intensity, as can be seen in the inset of Fig. 10, where the spectrally integrated and normalized waveguide output is plotted as a function of excitation. Above the lasing threshold of $2.2 \text{ MW}/\text{cm}^2$ the integrated emission intensity increases linearly with excitation until saturation is observed above $4 \text{ MW}/\text{cm}^2$. The waveguide output spectra in Fig. 10 shows that we indeed observe the ring cavity modes imprinted by the waveguide structure. In agreement with the ring diameter of 35 μm we find a mode separation of 1.7 nm. The envelope of the output corresponds in good approximation to the spectral profile of the optical gain in Fig. 3. The emission starts between 620 and 632 nm, where the highest gain is observed. For higher excitation the emission spectrum becomes broader with a larger extension to higher photon energies. For excitation below $2.2 \text{ MW}/\text{cm}^2$ the emission intensity is several orders of magnitude smaller.

In the spectrum, cavity modes with the same spacing of 1.7 nm can be seen. However, the envelope now reflects the low-density PL of the polymer (curve i in Fig. 2).

Since in the case of nanosecond excitation the exciting pulse is much longer than the exciton lifetime, we are operating here in a quasi-steady-state regime. To get a comparison with the femtosecond experiments, the respective excitation in watts per square centimeter has to be multiplied by the exciton lifetime τ_{exc} . Using $\tau_{\text{exc}} = 60$ ps,¹⁰ the threshold corresponds approximately to $130 \mu\text{J}/\text{cm}^2$ excitation fluence in the femtosecond regime, which is slightly larger than for the other cavities. However, this kind of structure is of particular interest, since it can be easily integrated and the emitted light can be coupled from the waveguide into an optical fiber.

6 Conclusions

In conclusion, we have demonstrated that stimulated emission and very large optical gain can be achieved in semiconducting conjugated polymers. The gain covers a spectral range of about 50 nm in a region where the polymer is transparent and can be as high as 10^4 cm^{-1} . Utilizing the large light amplification in the polymer, we obtain laser action for various integrated planar and microring cavities.

Acknowledgment

This work was supported by the U.S. Office of Naval Research (ONR) through the MURI Center for Advanced Multifunctional Nonlinear Optical Polymers and Molecular Assemblies (CAMP), by the U.S. National Science Foundation (NSF), and by an AFOSR/BMDO AASERT student program. The authors thank the Technical Research Center of Finland for providing the waveguide ring resonator substrates.

References

1. N. Tessler, G. J. Denton, and R. H. Friend, "Lasing from conjugated-polymer microcavities," *Nature* **382**, 695–697 (1996).
2. F. Hide, M. A. Diaz-Garcia, B. J. Schwartz, M. R. Andersson, Q. Pei, and A. J. Heeger, "Semiconducting polymers: a new class of solid-state laser materials," *Science* **273**(5283), 1833–1836 (1996).
3. H. J. Brouwer, V. V. Krasnikov, A. Hilberer, and G. Hadziionnon, "Blue superradiance from neat semiconducting alternating copolymer films," *Adv. Mater.* **8**(11), 935–937 (1996).
4. S. V. Frolov, W. Gellermann, M. Ozaki, K. Yoshino, and Z. V. Vardeny, "Cooperative emission in pi-conjugated polymer thin films," *Phys. Rev. Lett.* **78**(4), 729–732 (1997).
5. M. A. Diaz-Garcia, F. Hide, B. J. Schwartz, M. D. McGehee, M. R. Andersson, and A. J. Heeger, "'Plastic' lasers: comparison of gain narrowing with a soluble semiconducting polymer in waveguides and microcavities," *Appl. Phys. Lett.* **70**(24), 3191–3193 (1997).
6. C. Spiegelberg, A. Schülzgen, B. Kippelen, and N. Peyghambarian, "Gain dynamics in conjugated polymers at room temperature," *Proc. 5th Intl. Workshop on Nonlinear Optics and Excitation Kinetics in Semiconductors (NOEKS)*, (1998) (also accepted for publication in *Phys. Stat. Sol. B*).
7. A. Schülzgen, C. Spiegelberg, M. M. Morrell, S. B. Mendes, B. Kippelen, and N. Peyghambarian, "Near-diffraction-limited laser emission from a polymer in a high finesse planar cavity," (accepted for publication in *Appl. Phys. Lett.*) (1998).
8. E. Harlev and F. Wudl, private communication.
9. I. B. Berlman, *Handbook of Fluorescence Spectra of Aromatic Molecules*, 2nd ed., Academic, New York (1971).
10. N. Peyghambarian, C. Spiegelberg, A. Schülzgen, S. Shaheen, and B. Kippelen, presented at SPIE Annual Meeting, San Diego, CA (1997).
11. B. Mollay, U. Lemmer, R. Kersting, R. F. Mahrt, H. Kurz, H. F. Kauffmann, and H. Bässler, "Dynamics of singlet excitations in conjugated polymers: poly(phenylenevinylene) and poly(phenylphenylenevinylene)," *Phys. Rev. B* **50**(15), 10769–10779 (1994).
12. G. R. Hayes, I. D. W. Samuel, and R. T. Phillips, "Exciton dynamics in electroluminescent polymers studied by femtosecond time-resolved photoluminescence spectroscopy," *Phys. Rev. B* **52**(16), R11569–R11572 (1995).
13. M. Kuwata-Gonokami, R. H. Jordan, A. Dodabalapur, H. E. Katz, M. L. Schilling, and R. E. Slusher, "Polymer microdisc and microring lasers," *Opt. Lett.* **20**(20), 2093–2095 (1995).
14. S. V. Frolov, M. Shkunov, Z. V. Vardeny, and K. Yoshino, "Ring microlasers from conducting polymers," *Phys. Rev. B* **56**(8), R4363–R4366 (1997).



Axel Schülzgen received his PhD in experimental physics from Humboldt University Berlin, Germany, in 1992. During 1992 to 1995 he was a research fellow at Trinity College, Dublin, Ireland, and at Humboldt University Berlin, Germany, and studied optical properties of low-dimensional semiconductor structures. In 1996, he joined the Optical Sciences Center at the University of Arizona as an assistant research scientist, where he worked in the area of laser spectroscopy of inorganic semiconductors and polymers. His current research interests include propagation of short laser pulses and organic light-emitting devices.



Christine Spiegelberg received her PhD in experimental physics from Humboldt University Berlin, Germany, in 1992 with a thesis about NLO effects in II-VI bulk semiconductors and quantum dots. She was a research fellow at the Humboldt University Berlin until 1993, when she went to the IPCMS/CNRS in Strasbourg, France, to study carrier diffusion and kinetics in semiconductors. She was a postdoctoral fellow at MIC in Lyngby, Denmark, in 1995, doing ultrafast spectroscopy on III-V MQWs and superlattices, and joined the Optical Sciences Center at the University of Arizona in 1996 as an assistant research scientist. Her current research is on optical gain in conjugated polymers and its application in organic semiconductor lasers.



Michael M. Morrell received his BS degree from the Oregon Institute of Technology in 1995. He is currently researching organic LEDs and polymer lasers at the University of Arizona's Optical Sciences Center as a MS student.



Sergio B. Mendes received his PhD degree from the Optical Sciences Center of the University of Arizona, where he currently works as an assistant research professor. His major scientific interests include multifunctional waveguides, spectroscopy of molecular monolayers, optical sensors, and thin-film interference filters.

Pierre-Marc Allemand received a PhD in organic chemistry in 1990 from the University of California, Santa Barbara. His graduate research focused on conducting polymers and organic ferromagnets. He is currently a principal scientist at Donnelly Corporation, Advanced Technology Center, in Tucson, AZ. His research interests are in electro-optical materials synthesis and electrochromic device fabrication.



Yutaka Kawabe received his BS degree in physics from Kyoto University (Japan) in 1982, MS in physics from Kyoto University in 1984, and PhD in electrical engineering from Osaka University (Japan) in 1993. He was a researcher at the Central Research Laboratories, Idemitsu Kosan Co., Ltd., Japan from 1984 to 1995. He is currently an assistant research scientist at the Optical Sciences Center of the University of Arizona and has accepted a position as an

assistant professor at Chitose Institute of Science and Technology (Japan) from 1998 on. His research interests include organic nonlinear optical materials, organic LEDs, and optical dynamics in organic media.

Makoto Kuwata-Gonokami received his BS degree in physics in 1980, his MS in physics in 1982, and his PhD in physics in 1985, all from the University of Tokyo. He was a research associate at the Department of Physics, Faculty of Science of the University of Tokyo, from 1983 to 1988, and lecturer at the Department of Applied Physics, Faculty of Engineering, from 1988 to 1990. He has been an associate professor since 1990. His research interests include optical properties of semiconductors, organic materials, nonlinear optics, and ultrafast phenomena.



Seppo Honkanen received his DiplEng and DrTech degrees in 1984 and 1988, respectively, from the Department of Electrical Engineering at the Helsinki University of Technology, Finland. From 1984 to 1988 he was a research scientist at the Semiconductor Laboratory of the Technical Research Center of Finland. From 1989 to 1995 he was with Nokia Research Center, Finland, where he developed glass integrated optical devices and fiber

amplifiers for optical communications. During 1991 to 1993, he

spent two years as an invited researcher at the Photonics Group of Montreal, performing research on integrated optics. In November 1995 he joined the Optical Sciences Center, University of Arizona, where he is an assistant research professor. His main research interests are in integrated optical components for communications and sensor applications.

Mahmoud Fallahi: Biography and photograph appear with the paper "Design and fabrication of circular grating coupled distributed Bragg reflector lasers."



Bernard Kippelen received his PhD in solid-state physics in 1990 from the University of Strasbourg. Since 1991, he has been *chargé de recherches* at the Centre National de la Recherche Scientifique. He is currently an assistant research professor at the Optical Sciences Center of the University of Arizona. His research interests center on the development and characterization of new nonlinear optical materials.

Nasser Peyghambarian received his PhD in solid-state physics, specializing in optical properties of semiconductors, from Indiana University, Bloomington, Indiana. He holds the chair of lasers and photonics at the Optical Sciences Center of the University of Arizona, where he is also a professor in the Department of Material Science and Engineering. He is a Fellow of the Optical Society of America and the American Physical Society. He has published over 250 publications in refereed journals, one textbook, six edited research books, and several book chapters.